Title
Synaptic input to dentate granule cell basal dendrites in a rat model of temporal lobe epilepsy

Journal
The Journal of Comparative Neurology, 509(2)

ISSN
1550-7149

Authors
Thind, Khushdev K
Ribak, Charles E
Buckmaster, Paul S

Publication Date
2008-07-10

DOI
10.1002/cne.21745

Published in final edited form as:
J Comp Neurol. 2008 July 10; 509(2): 190–202. doi:10.1002/cne.21745.

Synaptic Input to Dentate Granule Cell Basal Dendrites in a Rat Model of Temporal Lobe Epilepsy*

Khushdev K. Thind[1], **Charles E. Ribak**[2], and **Paul S. Buckmaster**[1,3]

[1]Department of Comparative Medicine, Stanford University, Stanford, California 94305

[2]Department of Anatomy and Neurobiology, University of California, Irvine, Irvine, California 92697

[3]Department of Neurology & Neurological Sciences, Stanford University, Stanford, California 94305

Abstract

In patients with temporal lobe epilepsy some dentate granule cells develop basal dendrites. The extent of excitatory synaptic input to basal dendrites is unclear, nor is it known whether basal dendrites receive inhibitory synapses. We used biocytin to intracellularly label individual granule cells with basal dendrites in epileptic pilocarpine-treated rats. An average basal dendrite had 3.9 branches, was 612 μm long, and accounted for 16% of a cell's total dendritic length. In vivo intracellular labeling and post-embedding GABA-immunocytochemistry were used to evaluate synapses with basal dendrites reconstructed from serial electron micrographs. An average of 7% of 1802 putative synapses were formed by GABA-positive axon terminals, indicating synaptogenesis by interneurons. Ninety three percent of the identified synapses were GABA-negative. Most GABA-negative synapses were with spines, but at least 10% were with dendritic shafts. Multiplying basal dendrite length/cell and synapse density yielded an estimate of 180 inhibitory and 2140 excitatory synapses per granule cell basal dendrite. Based on previous estimates of synaptic input to granule cells in control rats, these findings suggest an average basal dendrite receives approximately 14% of the total inhibitory and 19% of excitatory synapses of a cell. These findings reveal that basal dendrites are a novel source of inhibitory input, but they primarily receive excitatory synapses.

Keywords

synapse; recurrent excitation; GABA; electron microscopy; dentate gyrus; hippocampus

Introduction

Temporal lobe epilepsy is the most common type of epilepsy in adults (Engel et al., 1997). In many patients with temporal lobe epilepsy the dentate gyrus displays abnormal features: loss of neurons in the hilus (Margerison and Corsellis 1966), including GABAergic interneurons (de Lanerolle et al., 1989), dispersion of granule cells (Houser, 1990), mossy fiber sprouting (Sutula et al., 1989), and possibly more granule cells with basal dendrites that extend into the hilus (Franck et al., 1995; von Campe et al., 1997). In some species,

*Supported by NIH/NINDS.

Corresponding author Paul Buckmaster, Department of Comparative Medicine, Stanford University, 300 Pasteur Drive, R321 Edwards Building Stanford, CA 94305-5342, (650)498-4774, (650)498-5085, psb@stanford.edu.
Associate editor: Joseph L. Price

including certain bats (Buhl and Dann, 1990) and monkeys (Seress and Mrzljak, 1987; Frotscher et al., 1988), a subpopulation of granule cells regularly has basal dendrites. In humans, basal dendrites normally extend into the hilus in 22-47% of granule cells (Seress and Mrzljak, 1987; Al-Hussain and Al-Ali, 1995; Lim et al., 1997; Lauer et al., 2003). Granule cell basal dendrites are more frequent in schizophrenics (Lauer et al., 2003), but that might be a side-effect of treatment with neuroleptics, which stimulate granule cell neurogenesis (Dawirs et al., 1998). Increasing the subpopulation of granule cells with basal dendrites might be pathogenic in patients with schizophrenia or epilepsy by augmenting positive-feedback circuits. Basal dendrites are ideally positioned to receive excitatory synaptic input from granule cell axons, which are concentrated in the hilus. In normal monkeys, granule cells with basal dendrites exhibit functional recurrent excitation (Austin and Buckmaster, 2004).

In adult rats and mice, virtually none of the granule cells in septal and middle parts of the hippocampus displays basal dendrites. However, granule cells with hilar basal dendrites develop after epileptogenic treatments (Spigelman et al., 1998; Buckmaster and Dudek, 1999; Dashtipour et al., 2003; Shapiro et al., 2005; Jakubs et al., 2006; Pekcec and Potschka, 2007; Walter et al., 2007). Ultrastructural evidence shows that hilar basal dendrites receive excitatory synaptic input (Ribak et al., 2000; Shapiro and Ribak, 2006; Jessberger et al., 2007; Shapiro et al., 2007). But the extent of excitatory input to these dendrites remains unclear. Nor is it known whether hilar basal dendrites receive inhibitory input. Both issues have important functional consequences. To address these questions we biocytin-labeled individual granule cells in epileptic pilocarpine-treated rats in vivo and in hippocampal slices, three-dimensionally reconstructed cells with hilar basal dendrites at the light microscopic level and basal dendrite segments at the electron microscopic level, and evaluated GABA-immunoreactivity of their presynaptic axons.

Methods

Pilocarpine-treated epileptic rats were prepared as described previously (Buckmaster, 2004). Briefly, 12 male Sprague-Dawley rats (Harlan, Indianapolis, IN) were treated with pilocarpine to induce status epilepticus when they were 45 ± 3 days old (mean ± s.e.m.). After 2 hrs of status epilepticus, rats received diazepam (10 mg/kg i.p.), which was repeated as needed to suppress seizures. In the following weeks rats were video-monitored to verify development of spontaneous seizures. Experiments were performed 74 ± 10 days after pilocarpine treatment. All procedures were in accordance with the National Institutes of Health Guide for the Care and Use of Laboratory Animals and approved by the Stanford University Institutional Animal Care and Use Committee.

Biocytin-labeled cells from a previous hippocampal slice study (Kobayashi and Buckmaster, 2003) were 3-dimensionally reconstructed using methods described previously (Buckmaster and Dudek, 1999). Briefly, horizontal 400-μm-thick slices were prepared from the temporal hippocampus. Granule cells were iontophoretically injected with biocytin with sharp intracellular electrodes in an interface recording chamber (Fine Science Tools, Foster City, CA). Slices were fixed in 4% paraformaldehyde in 0.1 M phosphate buffer (pH 7.4), cryoprotected in 30% sucrose in 0.1 M phosphate buffer, sectioned with a microtome set at 60 μm, and processed for visualization using the ABC method (Vector Laboratories, Burlingame, CA) and diaminobenzidine as the chromogen. Cells were chosen for reconstruction based on the presence of a basal dendrite and completeness of their dendritic tree, although some amputation of dendritic processes during slice preparation is possible. A Neurolucida system (MicroBrightField, Williston, VT) was used to 3-dimensionally reconstruct cells and measure dendritic length, which was not adjusted for shrinkage. Dendritic length measurements should therefore be considered as underestimates.

Two additional granule cells were labeled in epileptic rats (one per rat) in vivo and prepared for electron microscopy with post-embedding GABA-immunocytochemistry as described previously (Buckmaster et al., 2002b). Briefly, rats were anesthetized (1.2 g/kg urethane i.p.), placed in a stereotaxic apparatus, and a sharp intracellular electrode was used to intracellularly record and iontophoretically label individual granule cells with biocytin. Rats received an overdose of urethane (2 g/kg i.p.) and were perfused with 2.5% paraformaldehyde and 1% glutaraldehyde in 0.1 M PB. Hippocampi were isolated, cryoprotected, slightly straightened, frozen, and sectioned transversely (i.e., perpendicular to the long axis of the straightened hippocampus) with a sliding microtome set at 40 μm. Tissue was processed for visualization using the ABC method (Vector Laboratories) and diaminobenzidine as the chromogen. Sections were postfixed with 1% OsO_4 in sodium cacodylate buffer (pH 7.2) for 1 hr, dehydrated in a series of ethanols, placed in propylene oxide, gradually transferred to pure Araldite/Eponate-12 (Ted Pella, Redding, CA), and flat-embedded between sheets of ACLAR at 60°C for 24 hr. Areas of interest on the flat-embedded tissue section were isolated and mounted on a blank epoxyresin capsule. Block faces were trimmed and ultrathin sections (55 nm) cut from re-embedded blocks with an ultramicrotome (Reichert Ultracut S, Leica, Vienna, Austria). Serial sections were collected on coated, nickel single-slot grids.

Post-embedding GABA immunocytochemistry was performed on ultrathin sections by blocking nonspecific labeling with 0.8% ovalbumin and 5% fetal calf serum in 0.05 M tris-buffered saline (pH 7.6) for 1 hr followed by incubation overnight in antiserum in blocking solution. The anti-GABA serum (1:120, product no. A 2052, Sigma, St. Louis, MO) was developed in rabbit using GABA conjugated to bovine serum albumin as the immunogen. The antibody was isolated from antiserum by immunospecific methods of purification and showed positive binding with GABA in a dot blot assay, and negative binding with bovine serum albumin (manufacturer's technical information). Grids were gently rinsed and then incubated in anti-rabbit colloidal gold (10 nm diameter, 1:80; Ted Pella) in 0.1% Triton X-100 and 0.05 M tris buffer (pH 8.2) for 90 min. Sections were post-stained with 2% aqueous uranyl acetate for 6 min and Sato's lead stain for 4 min and then viewed and photographed using a transmission electron microscope (JEOL 100CX; JEOL, Peabody, MA).

Basal dendrites were reconstructed from electron micrographs of serial sections. Some of these were obtained at low magnification (2,500-7,500X) and used to align images that were taken at 25,000X with a final magnification after printing of 58,300X. Contours of low-magnification images were aligned with surrounding landmarks and served as a frame-of-reference for contour data collected at high magnification. Reconstruction was done using Neurolucida software (MicroBrightField) and a data tablet (Summagraphics, Seymour, CT). Three-dimensional dendrite length was not adjusted for shrinkage, and dendritic length measurements were determined only for reconstructed spans, not including gaps. Densities of spines and synapses were calculated by dividing numbers of each by dendritic length. Both spines and synapses were identified at the electron microscopic (EM) level, and dendritic length was measured at the EM level.

Synapses were identified by parallel membranes, concentration of presynaptic vesicles, presynaptic densities, and postsynaptic densities (Gray, 1959), when those were not obscured by electron dense reaction product in biocytin-labeled basal dendrites. Spines were identified as protuberances extending from the shaft, without regard for synaptic input. GABA-immunoreactive structures were identified by comparing densities of gold particles to background levels. Brightness and contrast of digital images were adjusted using Photoshop (Adobe, San Jose, CA).

Results

Granule cells (n=13) in hippocampal slices from epileptic rats were labeled with biocytin to reveal their dendritic tree. All had one basal dendrite and one or two apical dendrites. Apical dendrites extended into the molecular layer, and basal dendrites extended into the hilus. Basal dendrites were spiny and larger in diameter than axons (Figure 1). The cumulative length of apical dendrites was 3100 ± 243 μm/cell (mean ± s.e.m., range 1824-4107 μm/cell). Apical dendrites had 14.2 ± 1.2 branches/cell (range 9-25 branches/cell). Basal dendrites were 612 ± 142 μm/cell (range 158-1735 μm/cell) with 3.9 ± 1.4 branches/cell (range 0-16 branches/cell). Basal dendrite length accounted for 16 ± 4% (range 4-49%) of a cell's total dendritic length.

In addition, two granule cells with hilar basal dendrites were observed in a 135-day-old naïve control rat (Figure 2). Basal dendrites in control rats are rare (Ramón y Cajal S. 1995), and the small sample size precludes statistical comparisons with epileptic rats. Cumulative lengths of apical dendrites were 3269 and 3792 μm/cell. Apical dendrites had 13 and 24 branches/cell. Basal dendrites were 119 and 187 μm/cell. Basal dendrites had 0 and 2 branches/cell, and their cumulative length accounted for only 3% and 5% of each cell's total dendritic length.

For electron microscopic analysis, two granule cells labeled in vivo from epileptic rats were used to reveal synapses on their hilar basal dendrites. In the first case, the cell body was in the inferior blade of the granule cell layer (Figure 3A). The cell's primary axon projected into stratum lucidum of the CA3 field, and axon collaterals extended from the hilus into the granule cell layer and molecular layer. The apical dendrite was 1645 μm with 10 branches. The basal dendrite was 414 μm with 2 branches and accounted for 20% of the cell's total dendritic length. A 164-μm-long segment of the basal dendrite (Figure 3B) was re-sectioned and 3-dimensionally reconstructed from serial electron micrographs (Figure 3C).

This EM-reconstructed basal dendrite (#1) displayed numerous spines of various shapes, ranging from some with a large spine head to others with virtually no spine head (Figure 4). Quantitative spine and synaptic data for basal dendrite #1 are listed in Table 1. Putative synapses were identified by parallel membranes, concentration of synaptic vesicles, and a presynaptic density, but the electron dense reaction product associated with biocytin in the labeled basal dendrite obscured postsynaptic densities. Almost 95% of the putative synapses were with GABA-negative, presumably glutamatergic, axon terminals. Sixty two percent of GABA-negative axon terminals synapsed with spine heads (Figures 5AB, 6, and 7) while the remaining 38% synapsed directly onto dendritic shafts (Figures 7 and 8). Dense concentrations of gold particles labeled GABA-positive structures, including some dendrites (Figure 7) and synaptic boutons (Figures 6A and 7A). Thirty one percent of GABA-positive axon terminals synapsed with spines that also received a synapse from a GABA-negative axon terminal (Figure 6A), and the rest (69%) synapsed with the dendritic shaft (Figure 7A).

The second EM-reconstructed basal dendrite (#2) extended from a granule cell soma in the inferior blade of the granule cell layer and was labeled less intensely with biocytin than basal dendrite #1 (Figure 3D). A nearby granule cell that also had been labeled confounded definitive identification of the axon of each cell. Nevertheless, biocytin-labeled axon collaterals were evident in the hilus, granule cell layer, and molecular layer, and two primary axons with mossy fiber boutons extended into stratum lucidum of CA3. The cell with a basal dendrite had 2 apical dendrites with 8 branches and a total length of 1524 μm. The basal dendrite was 494 μm, which accounted for 24% of the cell's total dendritic length. At the light microscopic level the basal dendrite appeared to have 3 branches (Figure 3DE). However, at the electron microscopic level a fourth branch was discovered that extended

perpendicularly into the depth of the section and had been largely obscured by the main trunk of the basal dendrite. Therefore, the actual basal dendrite length was >494 μm.

A segment of this basal dendrite (#2) was 3-dimensionally reconstructed from serial electron micrographs (Figure 3F). As for basal dendrite #1, basal dendrite #2 displayed a range of spine sizes and shapes, and there were similarities in synaptic input (Table 1). Most synapses of basal dendrite #2 were formed by axon terminals that were GABA-negative (91%) but some were GABA-positive (9%). Overall, the most common synapse was between a GABA-negative axon terminal and a spine (Figures 5CD, 6CD, 9, and 10). GABA-positive axon terminals synapsed most frequently with dendritic shafts (72%) (Figure 10), but 28% of their synapses were with spines that also received a GABA-negative synapse (Figure 6CD). Spine synapses were most frequently with GABA-negative axon terminals (97%), but 3% were with GABA-positive terminals.

Basal dendrite #2 received a lower percentage of synapses with the dendritic shaft than basal dendrite #1, especially GABA-negative shaft synapses, although many were observed, and postsynaptic densities clearly were evident (Figure 9). Only 16% of all synapses were with the shaft, versus 40% for basal dendrite #1. Of GABA-negative synapses, only 10% were with the shaft, versus 38% for basal dendrite #1. The differences might be attributable to overestimation of GABA-negative shaft synapses in basal dendrite #1. In basal dendrite #2 postsynaptic densities were more evident and less obscured by reaction product. Therefore, synapses were identified with the aid of postsynaptic features, unlike basal dendrite #1, in which synapses were identified based only on presynaptic characteristics. In basal dendrite #2 electron dense reaction product was notably lighter in the heads of some spines compared to the shaft (Figures 5CD, 6CD, and 9). Although it facilitated visualization of postsynaptic densities, the lighter labeling of basal dendrite #2 made identification of biocytin-labeled dendrite profiles more difficult and resulted in more gaps in the reconstruction, including gaps between some spine heads and the shaft.

Figure 11 illustrates both EM-reconstructed basal dendrite segments and indicates sites and types of synapses. In both, the vast majority of synapses are GABA-negative spine synapses. GABA-positive synapses are scattered across the lengths of the reconstructed segments. In basal dendrite #2, synapse density appears lower at distal compared to proximal sites.

Discussion

The principal findings of the present study are that in an animal model of temporal lobe epilepsy basal dendrites receive inhibitory input and a high density of excitatory synapses on both spines and the shaft of these basal dendrites.

Comparisons with previous studies

Except for their unusual position in the hilus, basal dendrites display many similarities with apical dendrites of normal granule cells. Basal dendrites have approximately 3 spines/μm and display a range of sizes and shapes, similar to granule cell apical dendrites that have been evaluated with electron microscopy in control rats (Hama et al., 1989; Trommald and Hulleberg, 1997). In the molecular layer of control rats, where apical dendrites extend, 7% of synapses are formed by GABA-positive axon terminals and 93% are by GABA-negative axon terminals (Halasy and Somogyi, 1993), which is quite similar to results of the present study on basal dendrites. Most GABA-positive synapses are with shafts of basal dendrites, although some are with spines, similar to apical dendrites (Fifkova et al., 1992; Halasy and Somogyi, 1993; Buckmaster et al., 2002a). Like apical dendrites, most synapses formed by GABA-negative axon terminals are with spines of basal dendrites.

Apical and basal dendrites also appear to display differences. Only 4% of glutamatergic synapses are with shafts of apical dendrites (Halasy and Somogyi, 1993). Basal dendrites may receive a higher proportion of putative excitatory synapses with the shaft. Intense biocytin-labeling and dense reaction product obscured postsynaptic densities in the first examined basal dendrite, which made synapse identification more challenging. Nevertheless, presynaptic features suggested the presence of many shaft synapses. In the less intensely biocytin-labeled second reconstructed basal dendrite, postsynaptic densities of shaft synapses were more visible, which made false-positives less likely. Even the more conservative estimate of the second EM-reconstructed basal dendrite suggests that the proportion of GABA-negative synapses made with shafts of basal dendrites (10%) may be higher than that of apical dendrites. However, more data are needed to test that prediction.

Previously, serial EM was used to reconstruct a segment of basal dendrite in p35 knock-out mice, which are epileptic and display granule cell dispersion and mossy fiber sprouting (Patel et al., 2004). In that case, 90% of GABA-negative synapses were with spines and 10% were with the shaft, similar to results of basal dendrite #2. In the mouse, however, densities of spines and synapses were lower than both basal dendrites in the present study. It is unclear why the results are different. One possibility is a species-specific difference. Another is that the knock-out mice express the mutation their entire life. In the present study, it is assumed that most basal dendrites did not develop until after an epileptogenic injury in adulthood, based on previous studies (Spigelman et al., 1998; Buckmaster and Dudek, 1999; Dashtipour et al., 2003; Jakubs et al., 2006; Pekcec and Potschka, 2007; Walter et al., 2007). Differences in the microenvironment of mature versus immature dentate gyrus at the time of granule cell basal dendrite growth might affect synaptogenesis and spine formation.

In the present study, for light microscopic analysis, granule cells were labeled in horizontal slices from temporal hippocampus and results on basal dendrite length and branching might be different for cells at other septotemporal levels. In control rats, rare granule cell basal dendrites have been observed in the temporal hippocampus (Kobayashi and Buckmaster, 2003) but not in more septal regions (Spigelman et al., 1998; Buckmaster and Dudek, 1999; Jakubs et al., 2006). Similarly, in the temporal pole of control rats, some granule cell axons normally extend into the molecular layer (Ribak and Peterson, 1991; Cavazos et al., 1992), but to a smaller degree than epileptic rats (Buckmaster and Dudek, 1997). Recurrent excitation through basal dendrites and mossy fiber projections into the molecular layer may contribute to the temporal pole's heightened excitability (Burnham, 1975; Racine et al., 1977; Gilbert et al., 1985; Bragdon et al., 1986). In the present study, the basal dendrite segments reconstructed at the EM level were from two epileptic rats, and synapse densities of basal dendrites in control rats remain unknown.

GABAergic axon sprouting and synaptogenesis

It has been proposed that after epileptogenic injuries, surviving GABAergic interneurons sprout axon collaterals and form new inhibitory synapses with granule cells (Babb et al., 1989). Most of the evidence for interneuron axon sprouting is based on increased visualization of immunocytochemically stained axons in tissue from patients (Mathern et al., 1995; Patrylo et al., 1999) and animal models of temporal lobe epilepsy (Davenport et al., 1990; Bausch and Chavkin, 1997; Mathern et al., 1997; André et al., 2001). In those studies, GABAergic axon sprouting was inferred from increased optical density in areas where immunocytochemically labeled axons were concentrated. However, mRNA and peptide levels of interneuron markers increase in the dentate gyrus after seizure activity (Feldblum et al., 1990; Wanscher et al., 1990; Shinoda et al., 1991; Schwarzer et al., 1995; Houser and Esclapez 1996). Therefore, more interneuron axons may be apparent in epileptic tissue because more antigen is expressed in pre-existing axons. Even if there were axon sprouting,

synaptogenesis does not necessarily follow. Lesion studies provide more direct evidence of inhibitory axon sprouting (Deller et al., 1995). Additional evidence of GABAergic synaptogenesis comes from EM analysis of tissue from patients with temporal lobe epilepsy (Wittner et al., 2001).

The findings of the present study support the hypothesis that GABAergic axons sprout and form novel synapses after epileptogenic injuries. It is also possible that some GABAergic terminals are granule cell axons (Sandler and Smith, 1991; Sloviter et al., 1996). We estimate that basal dendrites receive 0.3 GABAergic synapses/μm, and the average basal dendrite is 612 μm, yielding approximately 180 inhibitory synapses/cell. Results of a previous GABA-immunocytochemistry EM study suggest that in control rats, each granule cell receives an average total of 1100 GABAergic synapses (Halasy and Somogyi, 1993). Basal dendrites, therefore, are likely to receive approximately 14% [180/(1100+180)] of a granule cell's inhibitory synapses.

The functional consequences of GABAergic axon sprouting and increased inhibitory input to basal dendrites are unclear. It might synchronize granule cell activity and lower seizure threshold (Babb et al., 1989; André et al., 2001). On the other hand, it might compensate for the loss of interneurons and inhibitory input to granule cells after epileptogenic injuries. Thus, augmenting or suppressing GABAergic axon sprouting might be a useful target for therapeutic intervention.

Estimating the extent of excitatory synaptic input to basal dendrites

In rat models of temporal lobe epilepsy, 5-31% of granule cells display basal dendrites (Spigelman et al., 1998; Buckmaster and Dudek, 1999; Ribak et al., 2000; Kobayashi and Buckmaster, 2003). If basal dendrites receive 3.5 glutamatergic synapses/μm, which is a conservative estimate from basal dendrite #2 of the present study, and the average basal dendrite is 612 μm, multiplying these two values yields approximately 2140 excitatory synapses per granule cell basal dendrite. Results of a previous study suggest that in control rats each granule cell receives an average total of 9400 glutamatergic synapses (Halasy and Somogyi, 1993). Basal dendrites, therefore, are likely to receive approximately 19% [2140/(9400+2140)] of a granule cell's excitatory synapses. Although some GABA-negative synapses with basal dendrites are likely to come from granule cells, others may arise from other types of glutamatergic neurons, including surviving mossy cells and CA3 pyramidal cells, both of which extend axon collaterals within the hilus (Buckmaster et al., 1993). Nevertheless, a substantial fraction of the total recurrent, excitatory circuit among granule cells may route through basal dendrites, which receive input from granule cells (Ribak et al., 2000; Patel et al., 2004), in addition to sprouted mossy fibers that synapse onto apical dendrites in the molecular layer (Buckmaster et al., 2002b). Consequently, to successfully prevent the development of aberrant positive-feedback circuits in the dentate gyrus after epileptogenic injuries, it may be necessary to block both axon sprouting into the molecular layer and growth of basal dendrites.

Acknowledgments

We are grateful to Ruth Yamawaki and Dr. Masayuki Kobayashi for technical assistance.

References

Al-Hussain S, Al-Ali S. A Golgi study of cell types in the dentate gyrus of the adult human brain. Cell Mole Neurobiol. 1995; 15:207–220.

André V, Marescaux C, Nehlig A, Fritschy JM. Alterations of hippocampal GABAergic system contribute to development of spontaneous recurrent seizures in the rat lithium-pilocarpine model of temporal lobe epilepsy. Hippocampus. 2001; 11:452–468. [PubMed: 11530850]

Austin JE, Buckmaster PS. Recurrent excitation of granule cells with basal dendrites and low interneuron density and inhibitory postsynaptic current frequency in the dentate gyrus of macaque monkeys. J Comp Neurol. 2004; 476:205–218. [PubMed: 15269966]

Babb TL, Pretorius JK, Kupfer WR, Crandall PH. Glutamate decarboxylase-immunoreactive neurons are preserved in human epileptic hippocampus. J Neurosci. 1989; 9:2562–2574. [PubMed: 2501460]

Bausch SB, Chavkin C. Changes in hippocampal circuitry after pilocarpine-induced seizures as revealed by opioid receptor distribution and activation. J Neurosci. 1997; 17:477–492. [PubMed: 8987772]

Bragdon AC, Taylor DM, Wilson WA. Potassium-induced epileptiform activity in area CA3 varies markedly along the septotemporal axis of the rat hippocampus. Brain Res. 1986; 378:169–173. [PubMed: 3742197]

Buckmaster PS. Laboratory animal models of temporal lobe epilepsy. Comp Med. 2004; 54:473–485. [PubMed: 15575361]

Buckmaster PS, Dudek FE. Neuron loss, granule cell axon reorganization, and functional changes in the dentate gyrus of epileptic kainate-treated rats. J Comp Neurol. 1997; 385:385–404. [PubMed: 9300766]

Buckmaster PS, Dudek FE. In vivo intracellular analysis of granule cell axon reorganization in epileptic rats. J Neurophysiol. 1999; 81:712–721. [PubMed: 10036272]

Buckmaster PS, Strowbridge BW, Schwartzkroin PA. A comparison of rat hippocampal mossy cells and CA3c pyramidal cells. J Neurophysiol. 1993; 70:1281–1299. [PubMed: 8283200]

Buckmaster PS, Yamawaki R, Zhang GF. Axon arbors and synaptic connections of a vulnerable population of interneurons in the dentate gyrus in vivo. J Comp Neurol. 2002a; 445:360–373. [PubMed: 11920713]

Buckmaster PS, Zhang GF, Yamawaki R. Axon sprouting in a model of temporal lobe epilepsy creates a predominantly excitatory feedback circuit. J Neurosci. 2002b; 22:6650–6658. [PubMed: 12151544]

Buhl EH, Dann JF. Basal dendrites are a regular feature of hippocampal granule cells in flying fox hippocampus. Neurosci Lett. 1990; 116:263–268. [PubMed: 2243603]

Burnham WM. Primary and transfer seizure development in the kindled rat. Can J Neurol Sci. 1975; 2:417–428. [PubMed: 1201529]

Cavazos JE, Golarai G, Sutula TP. Septotemporal variation of the supragranular projection of the mossy fiber pathway in the dentate gyrus of normal and kindled rats. Hippocampus. 1992; 2:363–372. [PubMed: 1308194]

Dashtipour K, Wong AM, Obenaus A, Spigelman I, Ribak CE. Temporal profile of hilar basal dendrite formation on dentate granule cells after status epilepticus. Epilepsy Res. 2003; 54:141–151. [PubMed: 12837565]

Davenport CJ, Brown WJ, Babb TL. Sprouting of GABAergic and mossy fiber axons in dentate gyrus following intrahippocampal kainite in the rat. Exper Neurol. 1990; 109:180–190. [PubMed: 1696207]

Dawirs RR, Hildebrandt K, Teuchert-Noodt G. Adult treatment with haloperidol increases dentate granule cell proliferation in the gerbil hippocampus. J Neural Transm. 1998; 105:317–327. [PubMed: 9660110]

de Lanerolle NC, Kim JH, Robbins RJ, Spencer DD. Hippocampal interneuron loss and plasticity in human temporal lobe epilepsy. Brain Res. 1989; 495:387–395. [PubMed: 2569920]

Deller T, Frotscher M, Nitsch R. Morphological evidence for the sprouting of inhibitory commissural fibers in response to the lesion of the excitatory entorhinal input to the rat dentate gyrus. J Neurosci. 1995; 15:6868–6878. [PubMed: 7472444]

Engel, J., Jr; Williamson, PD.; Wieser, HG. Mesial temporal lobe epilepsy. In: Engel, J., Jr; Pedley, TA., editors. Epilepsy: a comprehensive textbook. Philadelphia: Lippincott-Raven; 1997. p. 2417-2726.

Feldblum S, Ackermann RF, Tobin AJ. Long-term increase of glutamate decarboxylase mRNA in a rat model of temporal lobe epilepsy. Neuron. 1990; 5:361–371. [PubMed: 1976015]

Fifkova E, Eason H, Schaner P. Inhibitory contacts on dendritic spines of the dentate fascia. Brain Res. 1992; 577:331–336. [PubMed: 1606504]

Franck JE, Pokorny J, Kunkel DD, Schwartzkroin PA. Physiologic and morphologic characteristics of granule cell circuitry in human epileptic hippocampus. Epilepsia. 1995; 36:543–558. [PubMed: 7555966]

Frotscher M, Kraft J, Zorn U. Fine structure of identified neurons in the primate hippocampus: a combined Golgi/EM study in the baboon. J Comp Neurol. 1988; 275:254–270. [PubMed: 2464627]

Gilbert M, Racine RJ, Smith GK. Epileptiform burst responses in ventral vs. dorsal hippocampal slices. Brain Res. 1985; 361:389–391. [PubMed: 4084805]

Gray EG. Axo-somatic and axo-dendritic synapses of the cerebral cortex: an electron microscope study. J Anat. 1959; 93:420–433. [PubMed: 13829103]

Halasy K, Somogyi P. Distribution of GABAergic synapses and their targets in the dentate gyrus of rat: a quantitative immunoelectron microscopic analysis. J Hirnforsch. 1993; 3:299–308. [PubMed: 8270784]

Hama K, Arii T, Kosaka T. Three-dimensional morphometrical study of dendritic spines of the granule cell in the rat dentate gyrus with HVEM stereo images. J Electron Microsc Tech. 1989; 12:80–87. [PubMed: 2760687]

Houser CR. Granule cell dispersion in the dentate gyrus of humans with temporal lobe epilepsy. Brain Res. 1990; 535:195–204. [PubMed: 1705855]

Houser CR, Esclapez M. Vulnerability and plasticity of the GABA system in the pilocarpine model of spontaneous recurrent seizures. Epilepsy Res. 1996; 26:207–218. [PubMed: 8985701]

Jakubs K, Nanobashvili A, Bonde S, Ekdahl CT, Kokaia Z, Kokaia M, Lindvall O. Environment matters: synaptic properties of neurons born in the epileptic adult brain develop to reduce excitability. Neuron. 2006; 52:1047–1059. [PubMed: 17178407]

Jessberger S, Zhao C, Toni N, Clemson GD Jr, Li Y, Gage FH. Seizure-associated, aberrant neurogenesis in adult rats characterized with retrovirus-mediated cell labeling. J Neurosci. 2007; 27:9400–9407. [PubMed: 17728453]

Kobayashi M, Buckmaster PS. Reduced inhibition of dentate granule cells in a model of temporal lobe epilepsy. J Neurosci. 2003; 23:2440–2452. [PubMed: 12657704]

Lauer M, Beckmann H, Senitz D. Increased frequency of dentate granule cells with basal dendrites in the hippocampal formation of schizophrenics. Psychiatr Res Neuroimag. 2003; 122:89–97.

Lim C, Blume HW, Madsen JR, Saper CB. Connections of the hippocampal formation in humans: I. The mossy fiber pathway. J Comp Neurol. 1997; 385:325–351. [PubMed: 9300763]

Margerison JH, Corsellis JAN. Epilepsy and the temporal lobes. Brain. 1966; 89:499–530. [PubMed: 5922048]

Mathern GW, Babb TL, Pretorius JK, Leite JP. Reactive synaptogenesis and neuron densities for neuropeptide Y, somatostatin, and glutamate decarboxylase immunoreactivity in the epileptogenic human fascia dentata. J Neurosci. 1995; 15:3990–4004. [PubMed: 7751960]

Mathern GW, Bertram EH III, Babb TL, Pretorius JK, Kuhlman PA, Sradlin S, Mendoza D. In contrast to kindled seizures, the frequency of spontaneous epilepsy in the limbic status model correlates with greater aberrant fascia dentate excitatory and inhibitory axon sprouting, and increased staining for *N*-methyl-d-aspartate, AMPA, and $GABA_A$ receptors. Neuroscience. 1997; 77:1003–1019. [PubMed: 9130782]

Patel LS, Wenzel HJ, Schwartzkroin PA. Physiological and morphological characterization of dentate granule cells in the p35 knock-out mouse hippocampus: evidence for an epileptic circuit. J Neurosci. 2004; 24:9005–9014. [PubMed: 15483119]

Patrylo PR, van den Pol A, Spencer DD, Williamson A. NPY inhibits glutamatergic excitation in the epileptic human dentate gyrus. J Neurophysiol. 1999; 82:478–483. [PubMed: 10400974]

Pekcec A, Potschka H. Newborn neurons with hilar basal dendrites hallmark epileptogenic networks. NeuroReport. 2007; 18:585–589. [PubMed: 17413662]

Racine R, Rose PA, Burnham WM. Afterdischarge thresholds and kindling rates in dorsal and ventral hippocampus and dentate gyrus. Can J Neurol Sci. 1977; 4:273–278. [PubMed: 597802]

Ramón y Cajal, S. Histology of the nervous system of man and vertebrates. Swanson, N.; Swanson, LW., translators. Vol. 2. New York: Oxford UP; 1995. p. 614-625.

Ribak CE, Peterson GM. Intragranular mossy fibers in rats and gerbils form synapses with the somata and proximal dendrites of basket cells in the dentate gyrus. Hippocampus. 1991; 1:355–364. [PubMed: 1669315]

Ribak CE, Tran PH, Spigelman I, Okazaki MM, Nadler JV. Status epilepticus-induced hilar basal dendrites on rodent granule cells contribute to recurrent excitatory circuitry. J Comp Neurol. 2000; 428:240–253. [PubMed: 11064364]

Sandler R, Smith AD. Coexistence of GABA and glutamate in mossy fiber terminals of the primate hippocampus: an ultrastructural study. J Comp Neurol. 1991; 303:177–192. [PubMed: 1672874]

Schwarzer C, Williamson JM, Lothman EW, Vezzani A, Sperk G. Somatostatin, neuropeptide Y, neurokinin B and cholecystokinin immunoreactivity in two chronic models of temporal lobe epilepsy. Neuroscience. 1995; 69:831–845. [PubMed: 8596652]

Seress L, Mrzljak L. Basal dendrites of granule cells are normal features of the fetal and adult dentate gyrus of both monkey and human hippocampal formations. Brain Res. 1987; 405:169–174. [PubMed: 3567591]

Shapiro LA, Figueroa-Aragon S, Ribak CE. Newly generated granule cells show rapid neuroplastic changes in the adult rat dentate gyrus during the first five days following pilocarpine-induced seizures. Eur J Neurosci. 2007; 26:583–592. [PubMed: 17686039]

Shapiro LE, Korn MJ, Ribak CE. Newly generated dentate granule cells from epileptic rats exhibit elongated hilar basal dendrites that align along GFAP-immunolabeled processes. Neuroscience. 2005; 136:823–831. [PubMed: 16344154]

Shapiro LA, Ribak CE. Newly born dentate granule neurons after pilocarpine-induced epilepsy have hilar basal dendrites with immature synapses. Epilepsy Res. 2006; 69:53–66. [PubMed: 16480853]

Shinoda H, Nadi NS, Schwartz JP. Alterations in somatostatin and proenkephalin mRNA in response to a single amygdala stimulation vs. kindling. Mol Brain Res. 1991; 11:221–226. [PubMed: 1684628]

Sloviter RS, Dichter MA, Rachinsky TL, Dean E, Goodman JH, Sollas AL, Martin DL. Basal expression and induction of glutamate decarboxylase and GABA in excitatory granule cells of the rat and monkey hippocampal dentate gyrus. J Comp Neurol. 1996; 373:593–618. [PubMed: 8889946]

Spigelman I, Yan X-X, Obenaus A, Lee Y-S, Wasterlain CG, Ribak CE. Dentate granule cells form novel basal dendrites in a rat model of temporal lobe epilepsy. Neuroscience. 1998; 86:109–120. [PubMed: 9692747]

Sutula T, Cascino G, Cavazos J, Parada I, Ramirez L. Mossy fiber synaptic reorganization in the epileptic human temporal lobe. Ann Neurol. 1989; 26:321–330. [PubMed: 2508534]

Trommald M, Hulleberg G. Dimensions and density of dendritic spines from rat dentate granule cells based on reconstructions from serial electron micrographs. J Comp Neurol. 1997; 377:15–28. [PubMed: 8986869]

von Campe G, Spencer DD, de Lanerolle NC. Morphology of dentate granule cells in the human hippocampus. Hippocampus. 1997; 7:472–488. [PubMed: 9347345]

Walter C, Murphy BL, Pun RYK, Spieles-Engemann AL, Danzer SC. Pilocarpine-induced seizures cause selective time-dependent changes to adult-generated hippocampal dentate granule cells. J Neurosci. 2007; 27:7541–7552. [PubMed: 17626215]

Wanscher B, Kragh J, Barry DI, Bolwig T, Zimmer J. Increased somatostatin and enkephalin-like immunoreactivity in the rat hippocampus following hippocampal kindling. Neurosci Lett. 1990; 118:33–36. [PubMed: 1979672]

Wittner L, Maglóczky Zs, Borhegyi Zs, Halász P, Tóth Sz, Eröss L, Szabó Z, Freund T. Preservation of perisomatic inhibitory input of granule cells in the epileptic human dentate gyrus. Neuroscience. 2001; 108:587–600. [PubMed: 11738496]

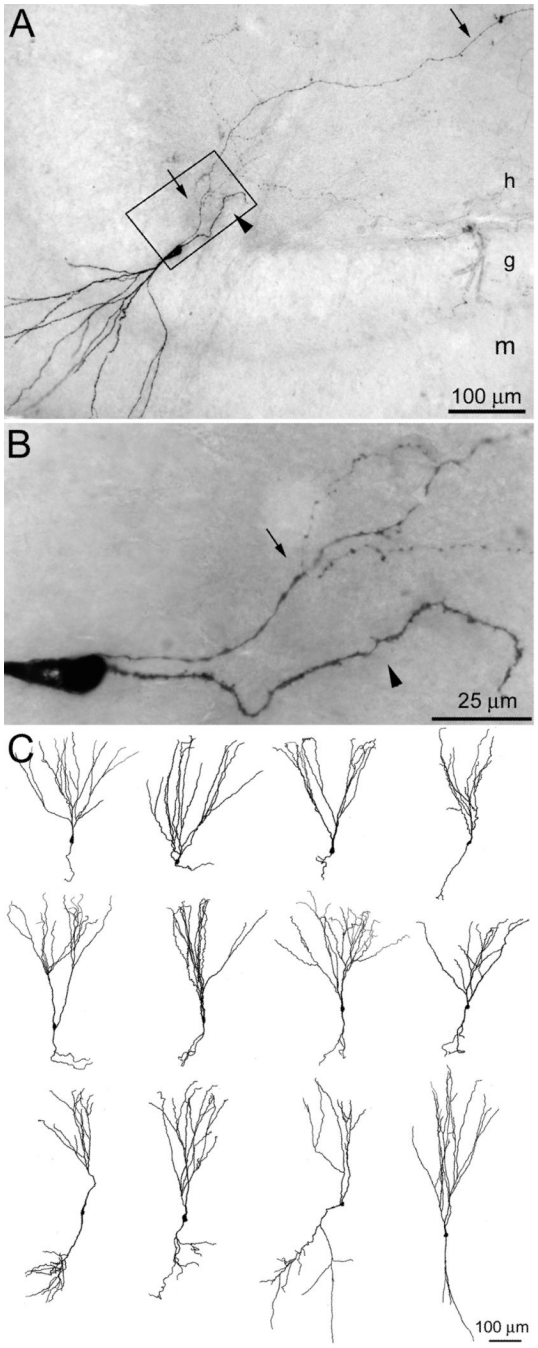

Figure 1.

Granule cells with basal dendrites in epileptic pilocarpine-treated rats. **A** Biocytin-labeled granule cell with an apical dendrite extending into the molecular layer (m) and a basal dendrite (arrow head) and axon (arrows) extending into the hilus (h). g = granule cell layer. **B** Magnified view of boxed region shown in **A**. The basal dendrite (arrow head) is larger in diameter and spiny. The axon (arrow) has fine-diameter collaterals and varicosities. **C** Reconstructions of granule cells with basal dendrites in epileptic rats. Basal dendrites project down, apical dendrites project up. Axons were not included in the reconstructions. The top-left reconstruction is of the cell shown in **A** and **B**.

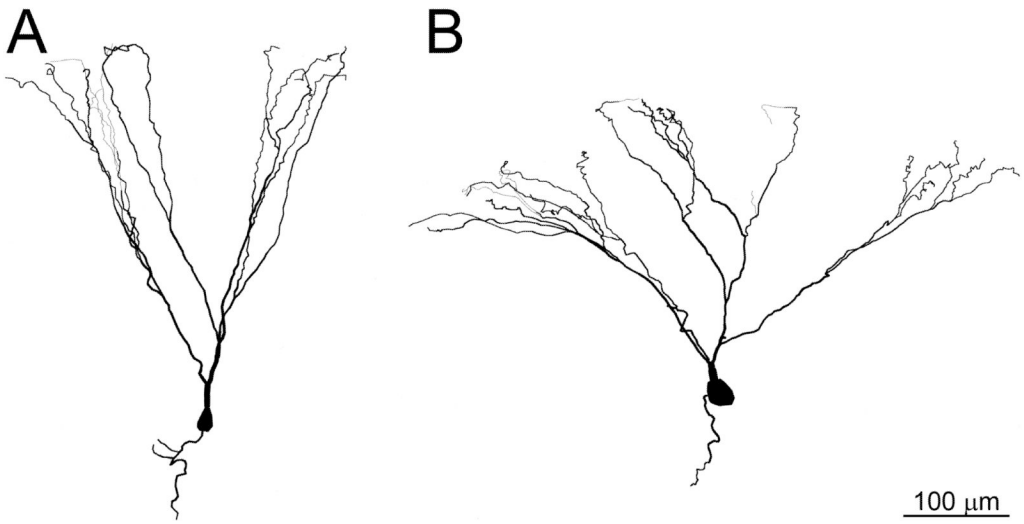

Figure 2.
Reconstructions of granule cells with basal dendrites in a control rat. Apical dendrites project up, basal dendrites project down.

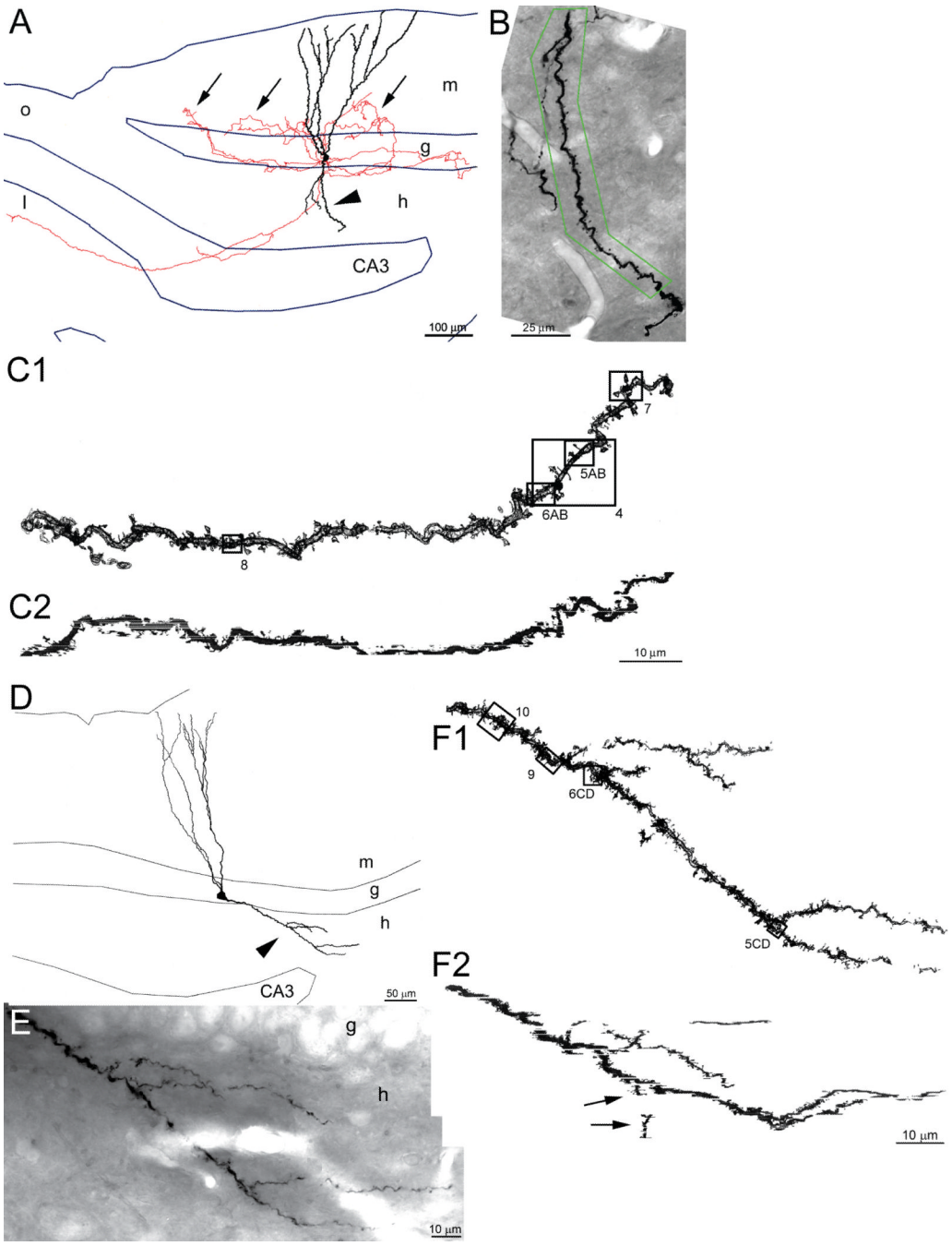

Figure 3.

Granule cells with a basal dendrites in epileptic rats that were used for electron microscopic reconstruction. **A** Reconstruction of granule cell #1. Dendrites are black; axon is red. Most dendrites extend into the molecular layer (m), but one basal dendrite (arrow head) projects into the hilus (h). The primary axon projects across the hilus and the CA3 pyramidal cell layer (CA3) and into stratum lucidum (l). Collaterals of the axon project through the granule cell layer (g) and into the molecular layer (arrows). o = stratum oriens of CA3. **B** Photomicrographic montage of basal dendrite #1 in one 40-µm-thick section. The segment of basal dendrite that was reconstructed from serial electron micrographs is indicated by the green contour. **C1** Reconstruction made from serial electron micrographs of the part of basal

dendrite #1 indicated by the green contour in **B**. Boxes indicate regions shown at high magnification in other figures. Numbers correspond to figures. **C2** Side view of the reconstructed segment of basal dendrite #1. **D** Reconstruction of granule cell #2. Most dendrites extend into the molecular layer, but one basal dendrite (arrow head) projects into the hilus. **E** Photomicrographic montage of basal dendrite #2 in one 40-μm-thick section. **F1** Reconstruction made from serial electron micrographs. Boxes indicate regions shown at high magnification to illustrate synapses. Numbers correspond to figures. **F2** Side view of the reconstructed segment of basal dendrite #2. Arrows indicate a branch (with a gap in the reconstruction) that extended perpendicularly into the depth of the section and was largely obscured by the main trunk of the basal dendrite in **E**.

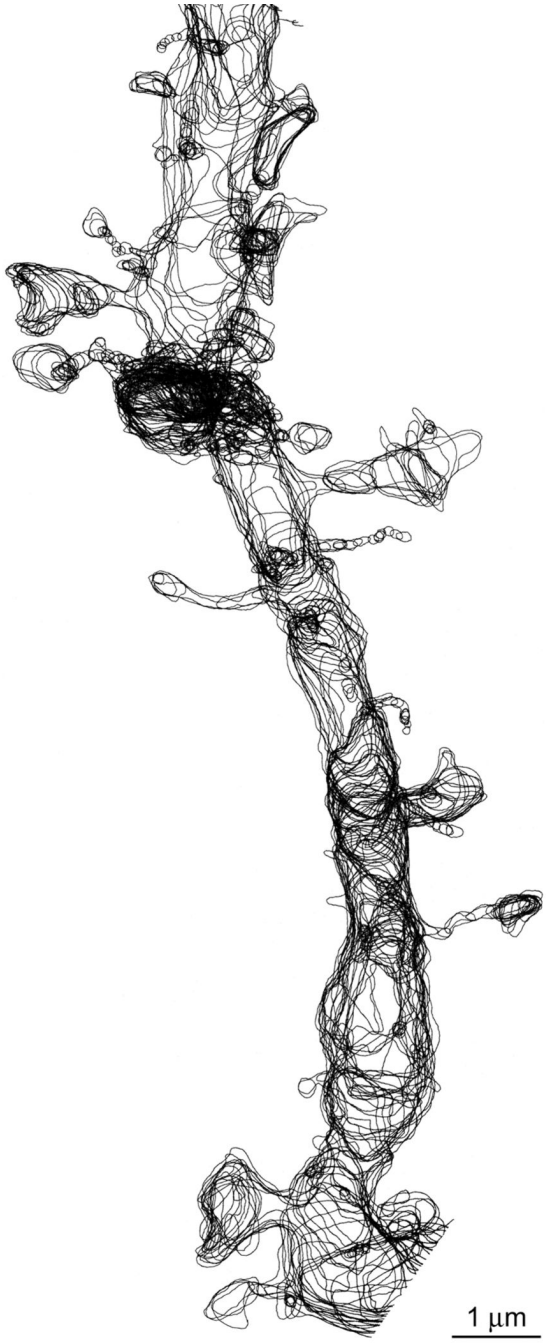

Figure 4.
Spines of a reconstructed segment of a granule cell basal dendrite in an epileptic rat display various shapes. This region corresponds to magenta box #4 in Figure 3C1.

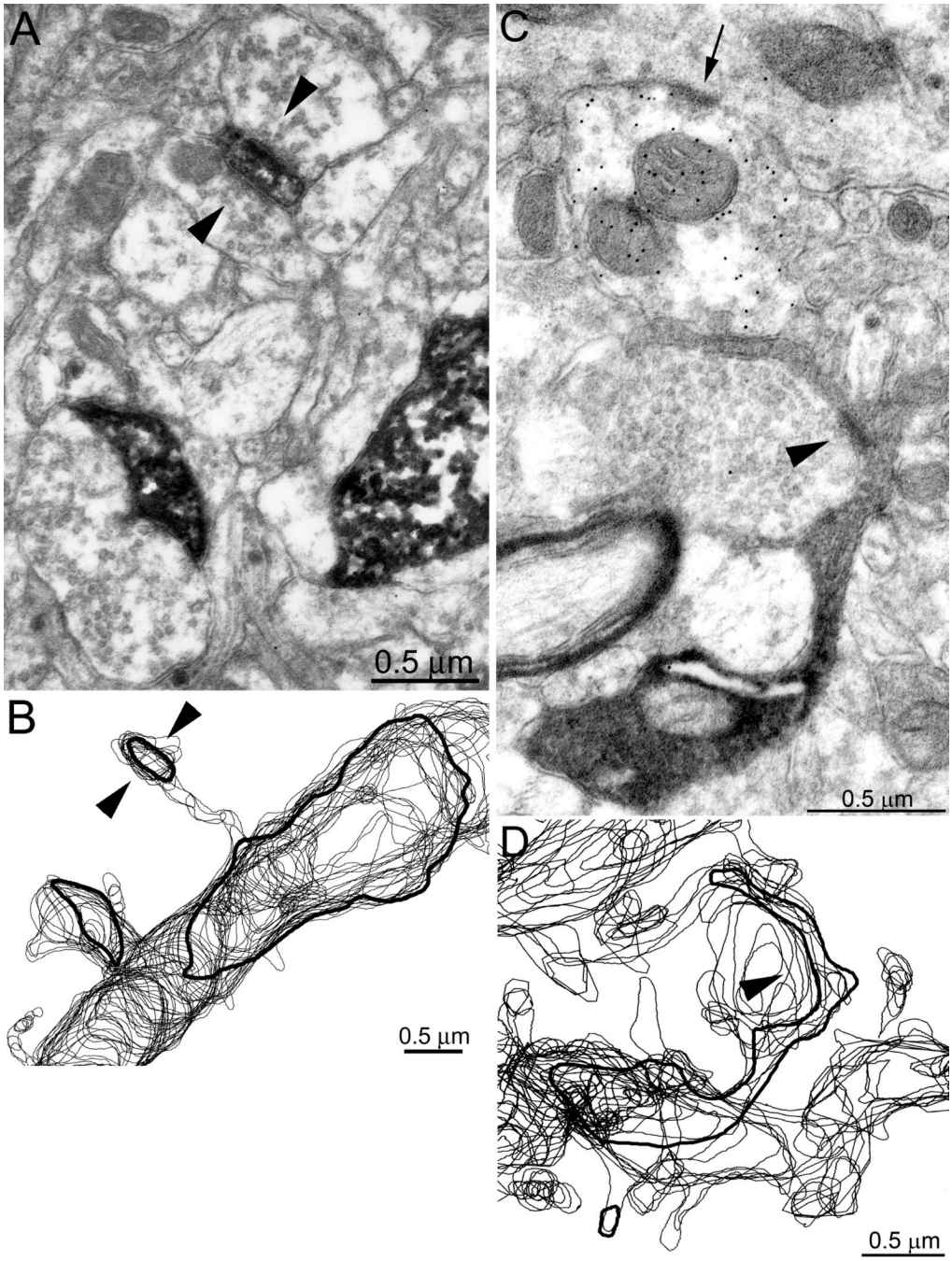

Figure 5.

GABA-negative synapses (arrowheads) with spines of granule cell basal dendrites in epileptic rats. **A** Electron micrograph of basal dendrite #1 and its detached spines (in this section) labeled with electron dense reaction product. **B** Reconstructed segment of basal dendrite #1. The bold contours are of the basal dendrite profile shown in **A**. This region corresponds to cyan box #5AB in Figure 3C1. **C** Electron micrograph of basal dendrite #2 labeled with electron dense reaction product, which is lighter in the spine head than in the shaft. Within the field of view a GABA-positive axon, labeled by 10-nm-diameter black colloidal-gold particles, synapses with a GABA-negative shaft (arrow). **D** Reconstructed

segment of basal dendrite. The bold contour is of the basal dendrite profile shown in **C**. This region corresponds to box #5CD in Figure 3F1.

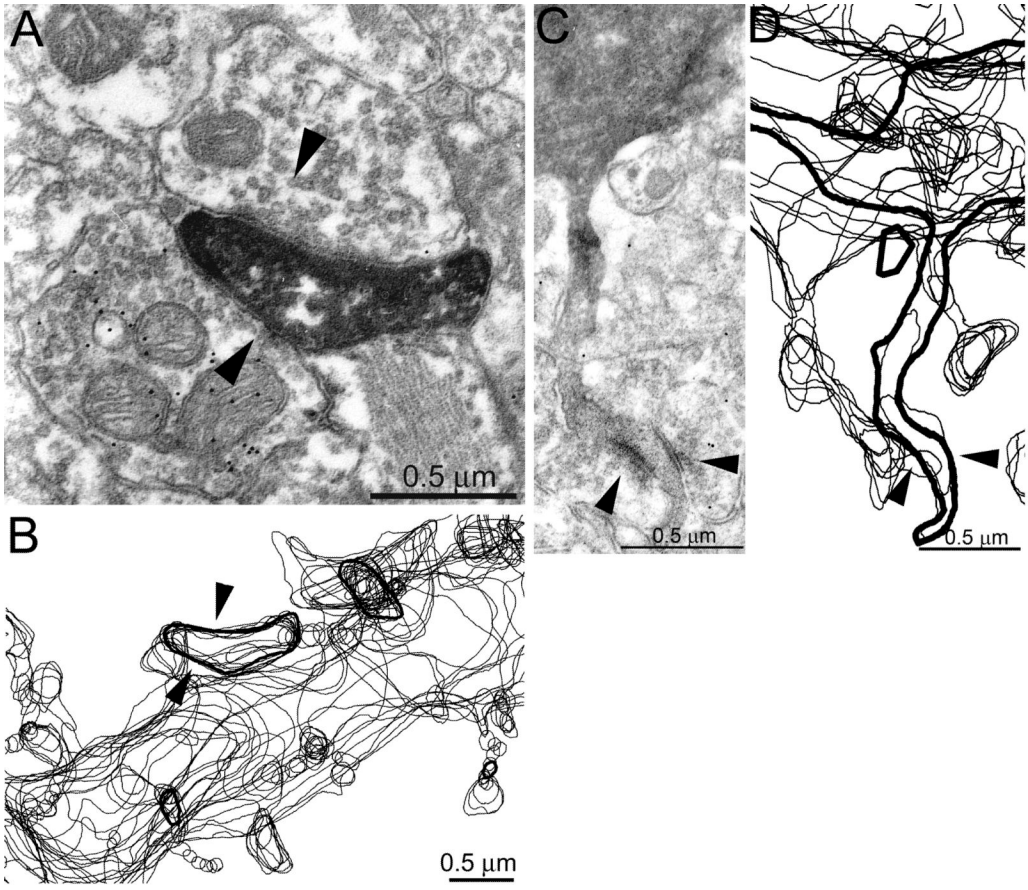

Figure 6.

GABA-negative and GABA-positive axon terminals synapse (arrowheads) with the same spine of granule cell basal dendrites in epileptic rats. **A** Electron micrograph of a spine of basal dendrite #1 labeled with electron dense reaction product. GABA-immunoreactivity is indicated by small black particles, which are 10-nm-iameter colloidal gold. **B** Reconstructed segment of basal dendrite #1. The bold contours are of the basal dendrite profile shown in **A**. This region corresponds to cyan box #6AB in Figure 3C1. **C** Electron micrographs of basal dendrite #2 labeled with electron dense reaction product, which is lighter in the spine head than in the shaft. GABA-immunoreactivity is indicated by small black particles, which are 10-nm-diameter colloidal gold. **D** Reconstructed segment of basal dendrite. The bold contours are of the basal dendrite profile shown in **C**. This region corresponds to box #6CD in Figure 3F1.

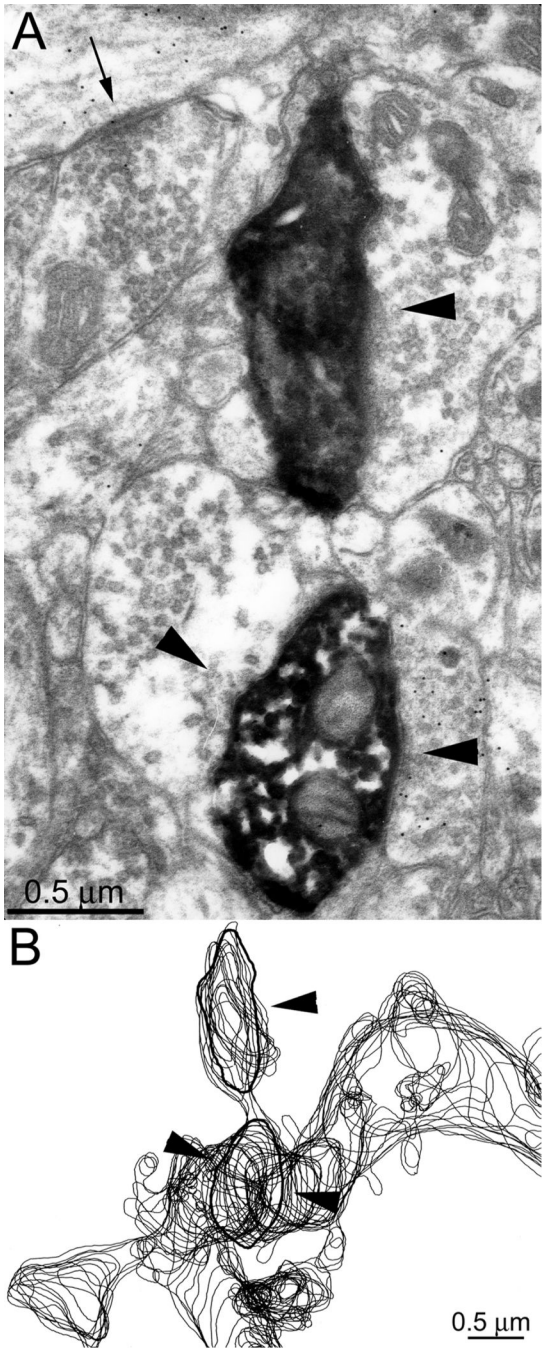

Figure 7.

Synapses (arrowheads) with a spine and shaft, including a GABA-positive synapse with the shaft of a granule cell basal dendrite in an epileptic rat. **A** Electron micrograph. The basal dendrite and its detached spine (in this section) are labeled with electron dense reaction product. GABA-immunoreactivity is indicated by small black particles, which are 10-nm-diameter colloidal gold. Within the field of view a GABA-negative axon synapses with a GABA-positive dendritic shaft (arrow). **B** Reconstructed segment of basal dendrite. The bold contours are of the basal dendrite profile shown in **A**. This region corresponds to cyan box #7 in Figure 3C1.

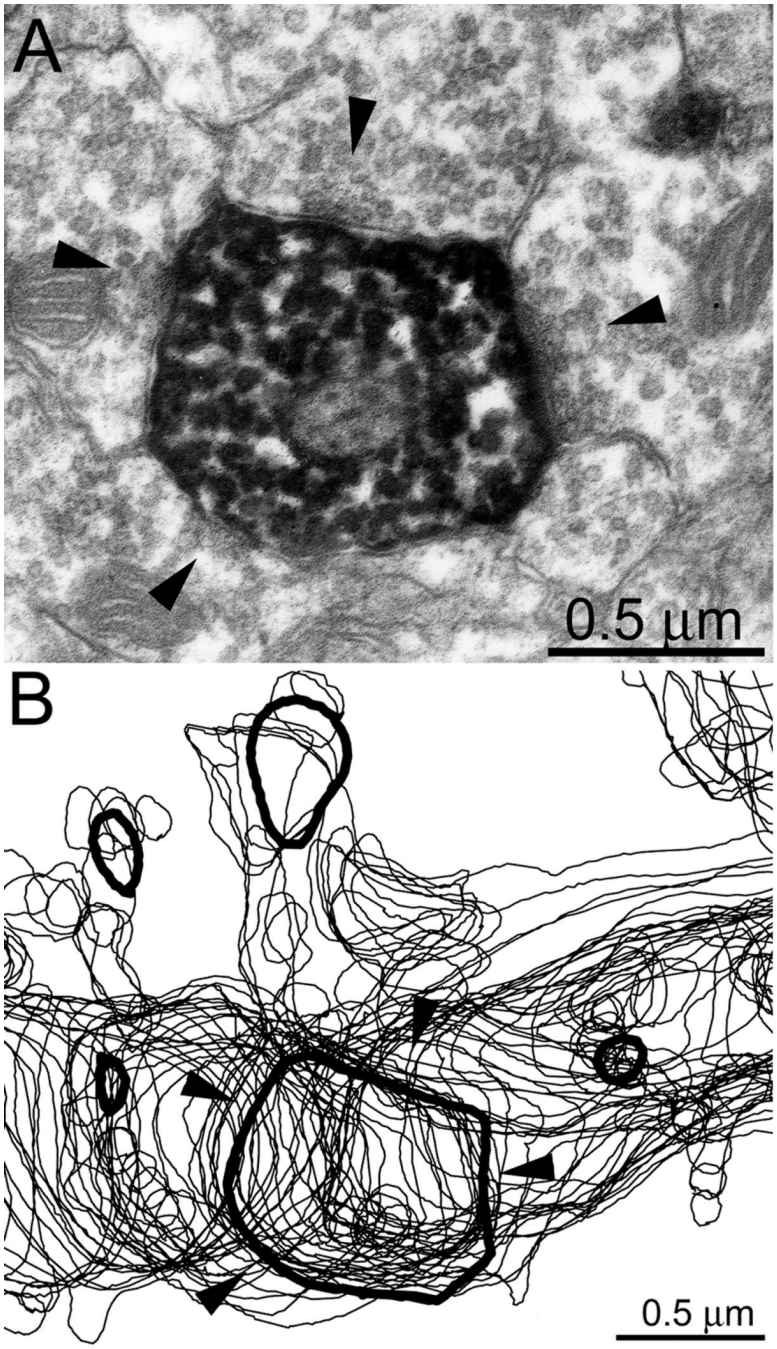

Figure 8.

Multiple GABA-negative synapses (arrowheads) with the shaft of a granule cell basal dendrite in an epileptic rat. **A** Electron micrograph. The basal dendrite is labeled with electron dense reaction product. **B** Reconstructed segment of basal dendrite. The bold contours are of the basal dendrite profile shown in **A**. This region corresponds to cyan box #8 in Figure 3C1.

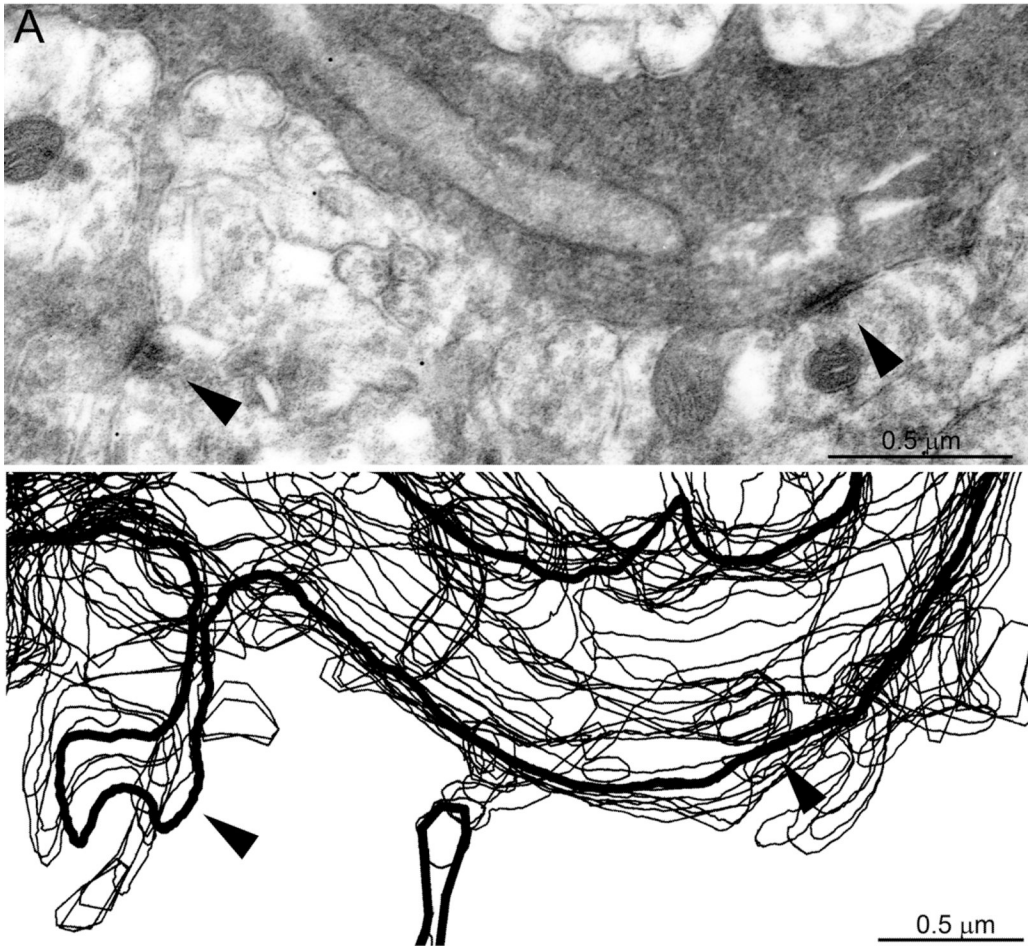

Figure 9.
GABA-negative synapses (arrowheads) with a spine and shaft of a granule cell basal dendrite in an epileptic rat. **A** Electron micrograph. The basal dendrite and its spine are labeled with electron dense reaction product, which is lighter in the spine head. **B** Reconstructed segment of basal dendrite. The bold contours are of the basal dendrite profile shown in **A**. This region corresponds to box #9 in Figure 3F1.

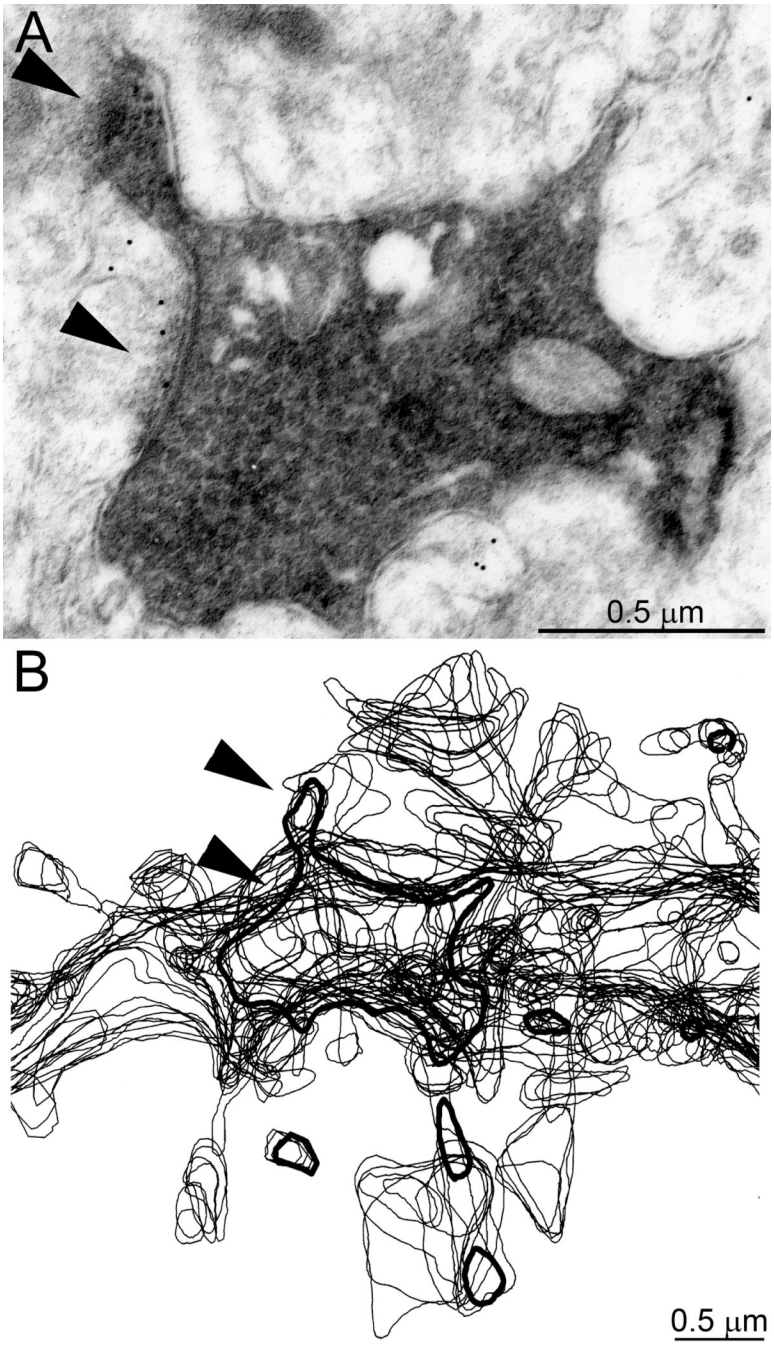

Figure 10.

Synapses (arrowheads) between a GABA-negative axon and a spine and between a GABA-positive axon and shaft of a granule cell basal dendrite in an epileptic rat. **A** Electron micrograph. The basal dendrite and its spine are labeled with electron dense reaction product. GABA-immunoreactivity is indicated by small black particles, which are 10-nm-diameter colloidal gold. **B** Reconstructed segment of basal dendrite. The bold contours are of the basal dendrite profile shown in **A**. This region corresponds to box #10 in Figure 3F1.

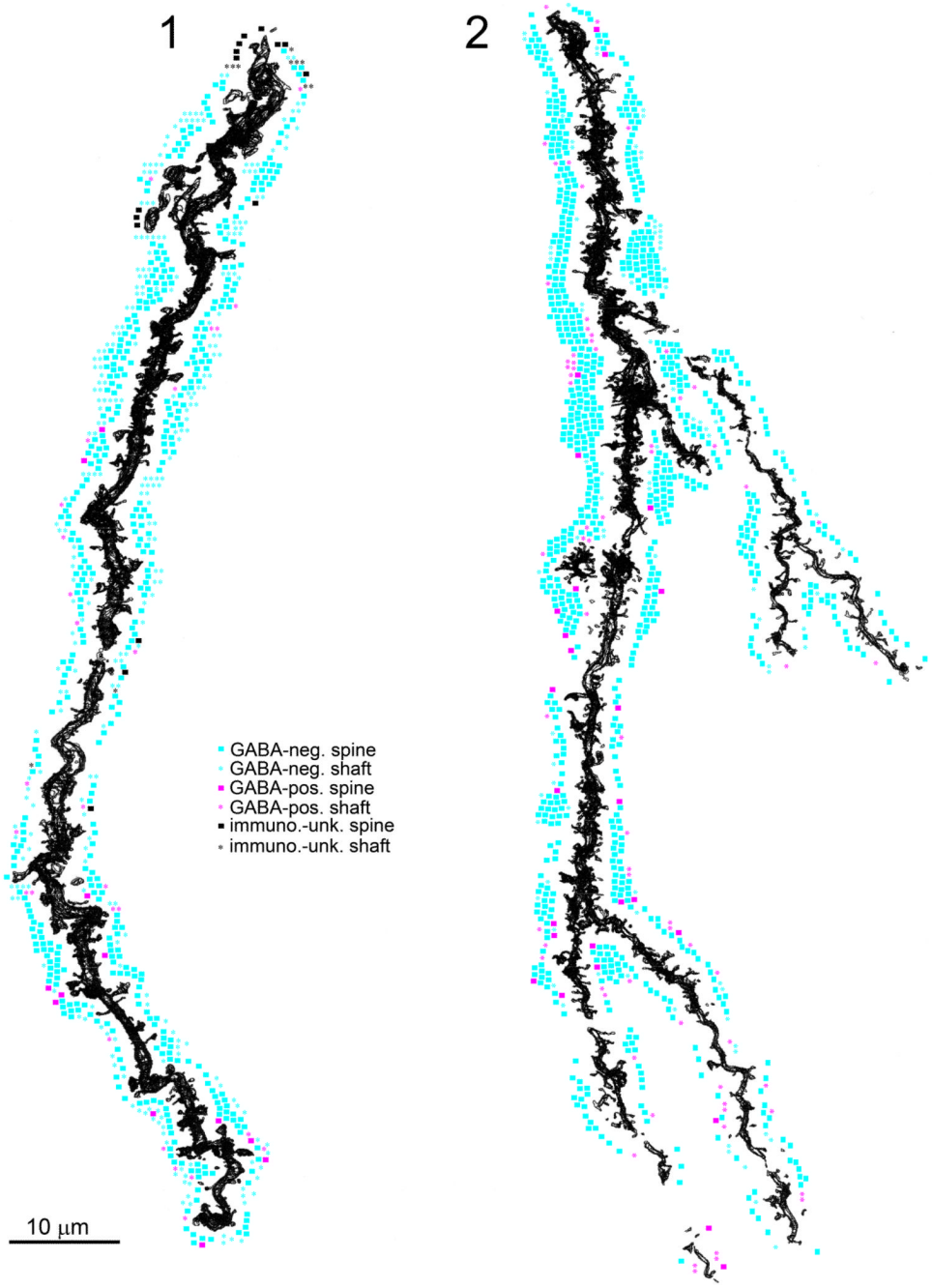

Figure 11.
Summary of synapses with granule cell basal dendrites #1 and #2 from epileptic rats. Proximal is up, distal is down. Synapses are indicated by markers. Most synapses are with GABA-negative spines. “Immuno.-unk.” synapses of basal dendrite #1 were in tissue sections that were used for the reconstruction but were not processed for immunocytochemistry.

Table 1

Granule cell basal dendrite segments in epileptic rats reconstructed from serial electron micrographs.

	basal dendrite #1	basal dendrite #2
# ultrathin sections	306	643
# micrographs	1893	2300
length (μm)	164	265
# synapses	773	1029
# GABA+ synapses	39	94
# GABA- synapses	708	935
# unknown synapses	26	0
# spine synapses	463	866
# shaft synapses	310	163
# GABA+ spine synapses	12	26
# GABA+ shaft synapses	27	68
# GABA- spine synapses	437	840
# GABA- shaft synapses	271	95